Cripto promotes A–P axis specification independently of its stimulatory effect on Nodal autoinduction

Daniela D'Andrea,[1] Giovanna L. Liguori,[1] J. Ann Le Good,[2] Enza Lonardo,[1] Olov Andersson,[2] Daniel B. Constam,[2] Maria G. Persico,[1] and Gabriella Minchiotti[1]

[1]Stem Cell Fate Laboratory, Institute of Genetics and Biophysics "A. Buzzati-Traverso," Consiglio Nazionale delle Ricerche, 80131 Naples, Italy
[2]Federal Institute of Technology Lausanne and Swiss Institute for Experimental Cancer Research, CH 1066 Epalinges, Switzerland

The *EGF-CFC* gene *cripto* governs anterior–posterior (A–P) axis specification in the vertebrate embryo. Existing models suggest that Cripto facilitates binding of Nodal to an ActRII–activin-like kinase (ALK) 4 receptor complex. Cripto also has a crucial function in cellular transformation that is independent of Nodal and ALK4. However, how ALK4-independent Cripto pathways function in vivo has remained unclear. We have generated *cripto* mutants carrying the amino acid substitution F78A, which blocks the Nodal–ALK4–Smad2 signaling both in embryonic stem cells and cell-based assays. In $cripto^{F78A/F78A}$ mouse embryos, Nodal fails to expand its own expression domain and that of *cripto*, indicating that F78 is essential in vivo to stimulate Smad-dependent Nodal autoinduction. In sharp contrast to *cripto*-null mutants, $cripto^{F78A/F78A}$ embryos establish an A–P axis and initiate gastrulation movements. Our findings provide in vivo evidence that Cripto is required in the Nodal–Smad2 pathway to activate an autoinductive feedback loop, whereas it can promote A–P axis formation and initiate gastrulation movements independently of its stimulatory effect on the canonical Nodal–ALK4–Smad2 signaling pathway.

Introduction

Cripto, a glycophosphatidylinositol (GPI)-linked membrane protein, is the founding member of a family of vertebrate signaling molecules, the EGF–Cripto-FRL1-Cryptic (CFC) family, which includes human, mouse, and chick Cripto (Ciccodicola et al., 1989; Dono et al., 1993; Colas and Schoenwolf, 2000), human and mouse Cryptic (Shen et al., 1997), *Xenopus laevis* FRL-1/XCR1, XCR2, and XCR3 (Kinoshita et al., 1995; Dorey and Hill, 2006; Onuma et al., 2006), and zebrafish one-eyed pinhead (oep; Zhang et al., 1998). During development, members of the EGF-CFC family are required for mesoderm and endoderm formation and patterning of the anterior–posterior (A–P) and left–right axes (Shen and Schier, 2000). Genetic studies and cell-based assays have shown that the EGF-CFC proteins stimulate signaling by the TGF-β–related Nodal (Shen and Schier, 2000). Moreover, receptor reconstitution experiments and coimmunoprecipitation assays suggest that Cripto interacts with Nodal and the activin type IB receptor (activin-like kinase [ALK] 4), thereby activating a complex with the activin type IIB serine/threonine kinase (ActRIIB) receptor (Reissmann et al., 2001; Yeo and Whitman, 2001; Bianco et al., 2002; Sakuma et al., 2002; Yan et al., 2002). Upon receptor activation, the intracellular kinase domain of the type I receptor phosphorylates Smad2 and/or Smad3, which form a hexameric complex with the common Smad4 and translocate into the nucleus to regulate gene expression in conjunction with other transcription factors such as FoxH1 (Massague and Chen, 2000; Adkins et al., 2003; Gray et al., 2003; Harrison et al., 2005). Similarly, Cripto can sensitize a complex of ActRIIB and ALK7 to Nodal (Reissmann et al., 2001), and it also interacts with a subset of related ligands such as GDF1 and 3 (Cheng et al., 2003; Chen et al., 2006). Furthermore, Cripto has been found to bind specific Nodal antagonists, such as the transmembrane protein tomoregulin-1 (TMEFF-1; Harms and Chang, 2003) or the TGF-β–related Lefty proteins (Chen and Shen, 2004). However, the structural determinants that mediate these diverse protein–protein interactions and their relative influence on specific signaling pathways in the embryo are poorly defined.

Consistent with an important role for *cripto* in Nodal signaling, loss-of-function analysis in the mouse has shown that *cripto* is essential for both primitive streak formation and conversion of the initial proximal-distal patterning into the A–P

Correspondence to Gabriella Minchiotti: minchiot@igb.cnr.it

Abbreviations used in this paper: A–P, anterior–posterior; ALK, activin-like kinase; ARE, activin response element; CFC, Cripto-FRL1-Cryptic; dpc, days past coitum; EB, embryoid body; ERK, extracellular signal-regulated kinase; ES, embryonic stem; GDF, growth/differentiation factor; GPI, glycophosphatidylinositol; oep, one-eyed pinhead.

The online version of this paper contains supplemental material.

The Journal of Cell Biology, Vol. 180, No. 3, February 11, 2008 597–605
http://www.jcb.org/cgi/doi/10.1083/jcb.200709090

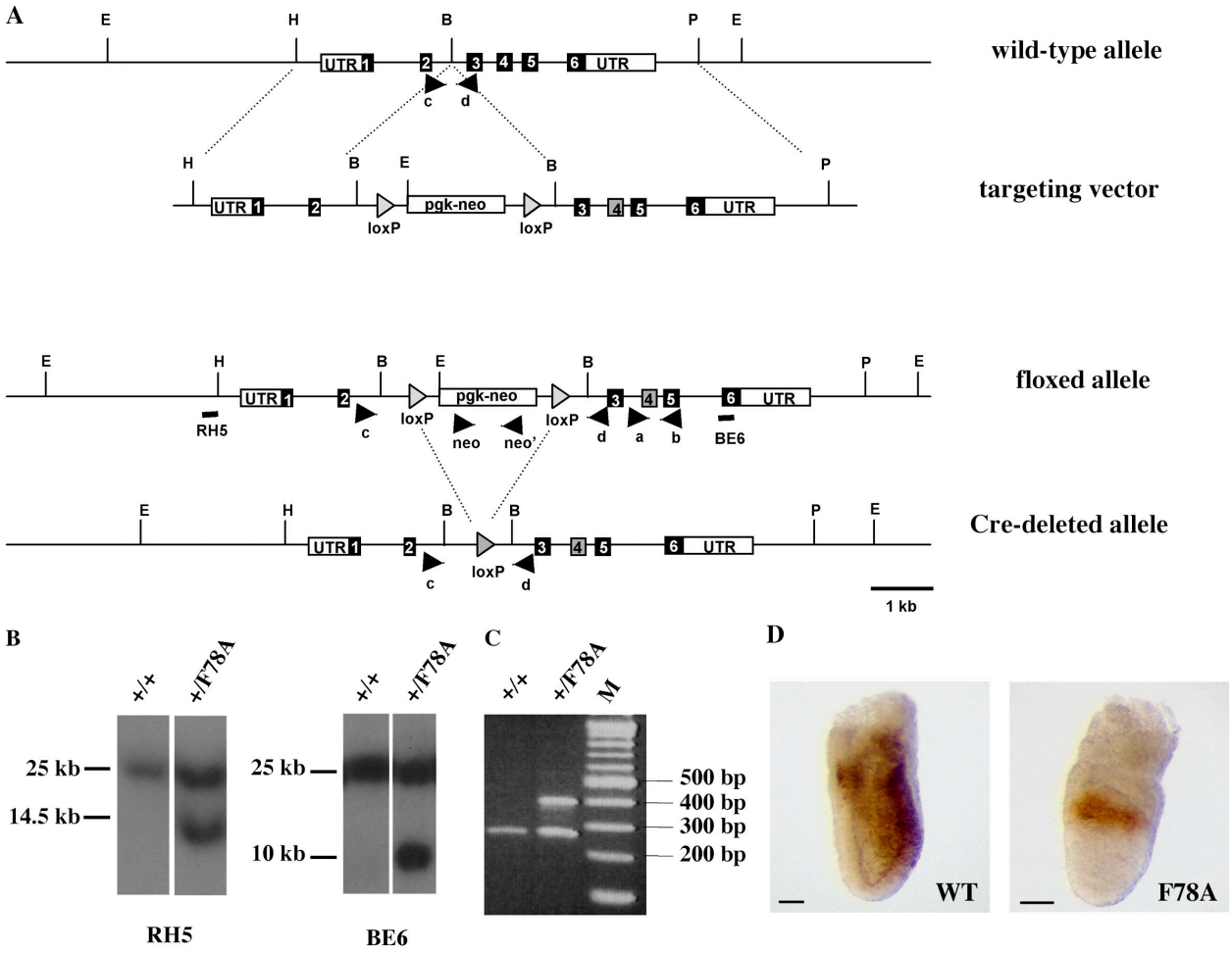

Figure 1. **Generation of *cripto*$^{F78A/F78A}$ mutant mice by homologous recombination in ES cells.** (A) Strategy for inserting the F78A substitution at the *cripto* locus. Numbered boxes represent wild-type exons (black) and the mutant exon carrying the F78A substitution (gray). Location of PCR primers (black arrowheads) and probes (black bars) used for genotyping are indicated. B, BamHI; E, EcoRV; H HindIII; P, PstI. (B) Genotyping of cell lines by Southern blot analysis. Genomic DNA from wild-type (+/+) and floxed (+/F78A) ES cells was digested with EcoRV and hybridized with the 5′ (RH5) and the 3′ (BE6) probes shown in A. The sizes of hybridized fragments are indicated in kilobases. (C) Genotypes of offspring from *cripto*$^{+/F78A}$ heterozygote intercrosses. Primers c and d amplified a 280-bp fragment of the wild-type allele and a 400-bp fragment of the Cre-deleted allele. (D) Spatial distribution of both wild-type (left) and F78A mutant (right) Cripto protein. Wild-type and *cripto*$^{F78A/F78A}$ embryos were immunostained with anti-Cripto antibodies at 6.75 dpc. Bars, 50 µm.

axis during gastrulation (Ding et al., 1998; Liguori et al., 2003). However, *cripto*-null embryos express posterior markers, such as *Brachyury* and *Fgf8*, and form anterior neural structures and extra-embryonic mesoderm, whereas *Nodal* mutants do not (Brennan et al., 2001). Thus, Nodal promotes anterior and posterior fates through both Cripto-dependent and -independent pathways.

Cripto has also been implicated in stimulating the progression of a broad spectrum of tumors (Salomon et al., 1999). Expression of *cripto* is increased severalfold in human colon, gastric, pancreatic, and lung carcinomas and in a variety of different types of mouse and human breast carcinomas (Ciardiello et al., 1991; Baldassarre et al., 1997). Although a specific receptor for Cripto has not yet been identified in mammary gland or cancer cells, mouse and human Cripto can activate a ras–raf–MAP kinase signaling pathway. This response may depend on the ability of Cripto to transactivate erbB-4 and/or FGF receptor 1 or to specifically bind to a membrane-associated heparan sulfate proteoglycan, glypican 1, leading to the activation of a Src-like tyrosine kinase (Bianco et al., 2003). However, without reagents that prevent endogenous Cripto from activating canonical ALK signaling, it has remained difficult to directly assess the physiological role of ALK-independent pathways.

Several structural determinants have been identified in the EGF and the CFC domains that regulate Cripto activity in cell transfection and *X. laevis* injection assays. Specifically, the CFC domain is essential for ALK4 interaction (Yeo and Whitman, 2001; Adkins et al., 2003), whereas threonine 72 in the EGF domain is *O*-fucosylated (Schiffer et al., 2001) and, apparently, promotes Nodal binding (Yeo and Whitman, 2001; Yan et al., 2002). It is worth noting that recent data indicate that the threonine residue that carries fucose, but not fucose per se, is required for Cripto to facilitate Nodal signaling (Shi et al., 2007). Furthermore, rescue experiments in *cripto*$^{-/-}$ mouse embryonic stem cells and in *oep* mutant zebrafish established that recombinant Cripto protein also relies on the conserved amino acid F78 (Minchiotti et al., 2001; Parisi et al., 2003). However, whether

Table I. **Genotypes of embryos and viable offspring from heterozygous intercrosses**

Stage	Number of litters analyzed	Number of animals obtained	Genotype (%)		
			+/+	+/F78A	F78A/F78A
E 6.5	35	220	32	48	20
E 7.5	45	304	20	49	31
E 8.5	33	221	20	47	33
E 9.5	4	30	22	51	27
E 10.5	3	26	18	48	34
E 11.5	4	40	25	70	5
E 12.5	4	40	33	67	0
From newborn to adult	100	602	35	65	0

E, embryonic day.

F78 is essential for all Cripto activities or whether it specifically promotes Nodal signaling has remained unclear.

In this paper, we provide direct evidence that Cripto^{F78A} is unable to activate detectable amounts of Smad2 in embryonic stem (ES) cell–derived embryoid bodies (EBs) and that it fails to stimulate canonical Nodal–ALK4–Smad2 signaling in cell-based luciferase reporter assays. Further analysis of *cripto*$^{F78A/F78A}$ mutant embryos confirms that residue F78 is essential to potentiate autoregulatory feedback signaling mediated by the Nodal–ALK4–Smad–FoxH1 pathway. We show that, unlike *cripto*-null mutants, *cripto*$^{F78A/F78A}$ embryos clearly establish an A–P axis and initiate germ layer formation and gastrulation movements. A subset of known Nodal effector genes that are down-regulated in *cripto*-null mutants are significantly induced in *cripto*$^{F78A/F78A}$ embryos. Collectively, these results suggest that Cripto can promote axis formation and gastrulation movements independently of its known stimulatory effect on the canonical Nodal–ALK4–Smad2 pathway.

Results

Cripto$^{F78A/F78A}$ mutants are embryonic lethal

To unravel the complex network of molecular interactions of Cripto with its target proteins in vivo, the amino acid residue F78, which is located in the EGF-like domain, was substituted by alanine (F78A) using Cre/loxP-mediated recombination (Fig. 1, A–C). The resulting heterozygous *cripto*$^{+/F78A}$ mice appeared phenotypically normal and were fertile; however, homozygosity for the *cripto*^{F78A}-targeted allele resulted in embryonic lethality. We first verified the expression of the mutated allele in vivo by whole-mount immunohistochemistry analysis. Cripto protein was consistently detected in homozygous *cripto*$^{F78A/F78A}$ embryos, although its expression remained confined to the proximal epiblast (Fig. 1 D). Although this result indicates that the alanine substitution does not abolish the synthesis or stability of Cripto protein, expansion of the expression domain to the distal epiblast is clearly compromised. Upon dissection, *cripto*$^{F78A/F78A}$ mutants were recovered at the expected mendelian ratio until 10.5 d past confluence (dpc) and later were resorbed (Table I). However, at 7.5 dpc they already displayed ectopic folds in the embryonic region (Fig. 2, A and A′). At 8.5 dpc, mutant embryos failed to turn and the neural folds were enlarged (Fig. 2, B and B′), apparently at the expense of mesodermal structures, because somites and a beating heart were absent. These results show that residue F78 of Cripto is essential for postimplantation development.

A–P axis and mesendoderm formation in cripto$^{F78A/F78A}$ mutants

Loss-of-function analysis has shown that *cripto* converts proximal-distal patterning into an A–P axis and promotes primitive streak formation (Ding et al., 1998; Liguori et al., 2003). To assess

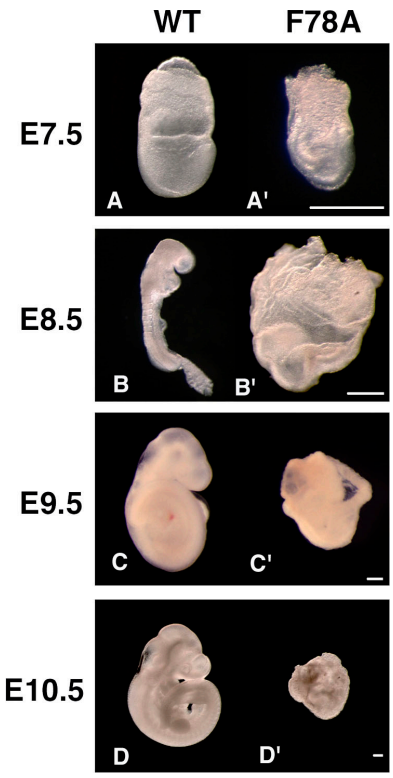

Figure 2. **Homozygous mutant *cripto*$^{F78A/F78A}$ embryos initiate gastrulation but subsequently arrest development.** Morphology of wild-type embryos (A–D) and *cripto*$^{F78A/F78A}$ mutant litter mates (A′–D′) dissected at 7.5 (A and A′), 8.5 (B and B′), 9.5 (C and C′), and 10.5 (D and D′) dpc. Both anterior and posterior structures that are absent in *cripto*-null mutants (Ding et al., 1998; Liguori et al., 2003) can be clearly recognized at up to 8.5 dpc but subsequently deteriorate (C′ and D′). Bars, 40 μm.

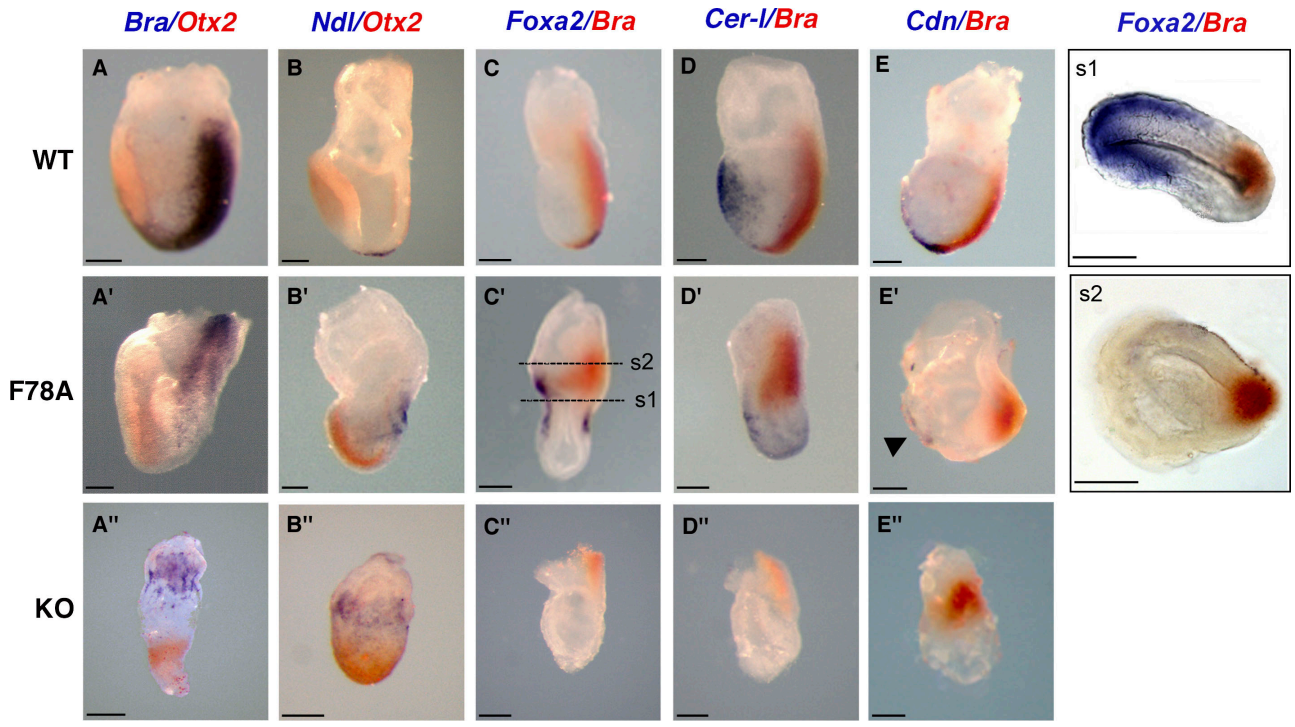

Figure 3. **Analysis of gastrulation defects in *cripto*$^{F78A/F78A}$ mutants reveals a hypomorphic phenotype.** Wild-type (top), *cripto*$^{F78A/F78A}$ (middle), and *cripto*-null (bottom) embryos at 7.5 dpc stained by whole-mount mRNA in situ hybridization. All embryos are shown with anterior side toward the left. (A, A′, and A″) Double staining of *Brachyury* (blue) and *Otx2* (red) mRNAs in the primitive streak and anterior neurectoderm, respectively, reveals normal A–P patterning in wild-type (A) and *cripto*$^{F78A/F78A}$ embryos (A′). In contrast, in *cripto*-null mutants (A″), cells expressing *Brachyury* and *Otx2* remain in the proximal and distal epiblast, respectively. (B, B′, and B″) Double staining for *Nodal* (blue) and *Otx2* (red) in wild-type embryos marks the node and the anterior neuroectoderm, respectively (B). In *cripto*$^{F78A/F78A}$ embryos (B′), *Nodal* mRNA is expressed in a group of posterior cells, whereas it is confined to the embryonic–extraembryonic boundary in *cripto*-null mutants (B″). (C, C′, and C″) Double staining of *Foxa2* (blue) and *Brachyury* (red). (C) *Foxa2* is expressed in the node and axial mesendoderm of wild-type embryos. (C′) In *cripto*$^{F78A/F78A}$ embryos, *Foxa2* marks both the distal primitive streak and the anterior side of the embryo. (C″) *Foxa2* is not expressed in *cripto*-null embryos. (D, D′, and D″) Double staining for *Cer-1* (blue) and *Brachyury* (red) reveals that *Cer-1* marks the anterior definitive endoderm in both wild-type (D) and *cripto*$^{F78A/F78A}$ (D′) embryos. In contrast, *Cer-1* expression is absent in *cripto*-null mutants (D″). (E, E′, and E″) Double staining for *Chordin* (blue) and *Brachyury* (red). *Chordin* marks the axial mesendoderm in wild-type (E) and *cripto*$^{F78A/F78A}$ (E′, arrowhead) embryos; however, the axial mesoderm is not expressed in *cripto*-null mutants (E″). (s1 and s2) Transverse sections taken from the embryo in C′. *Foxa2* signal is localized throughout the anterior proximal region of the embryo, revealing the presence of mesoderm and definitive endoderm (s1). *Brachyury* expression is confined to posterior embryonic and extraembryonic mesoderm. Bars, 50 μm.

whether *cripto*$^{F78A/F78A}$ embryos have defects in axis formation, we examined the expression of asymmetrically expressed marker genes such as *Brachyury* and *Otx2* at 7.5 dpc. In normal embryos, *Brachyury* marks the primitive streak, whereas expression of the anterior neural marker *Otx2* by this stage is restricted to the opposite pole (Fig. 3 A; Wilkinson et al., 1990; Simeone et al., 1993). By comparison, *cripto*-null mutants largely consist of anterior neuroectoderm (Ding et al., 1998; Liguori et al., 2003) and, therefore, ectopically express Otx2 throughout the distal embryonic region (Fig. 3 A″; Ding et al., 1998; Liguori et al., 2003), whereas the mesodermal marker *Brachyury* is only activated in a few cells along the embryonic–extraembryonic boundary (Fig. 3 A″; Ding et al., 1998). In contrast, in *cripto*$^{F78A/F78A}$ mutant embryos, *Brachyury* expression was normally posteriorized and persisted until 8.5 dpc, indicating the presence of posterior mesoderm populations that are missing in *cripto*-null mutants (Fig. 3 A′; and Fig. S1, A, A′, and A″, available at http://www.jcb.org/cgi/content/full/jcb.200709090/DC1). In addition, *Otx2* mRNA was consistently localized in the anterior region (Fig. 3 A′; and Fig. S1, A and A′), suggesting that A–P patterning is relatively normal. To monitor posterior neuroectoderm, we also analyzed the expression of *Krox20*, a marker of rhombomeres three and five, which is absent in *cripto*-null mutants (Ding et al., 1998). *Krox20* mRNA was clearly detected in *cripto*$^{F78A/F78A}$ embryos at 8.5 dpc (Fig. S1, B and B′). In addition, *Mox1*, a marker of paraxial mesoderm that fails to be induced in *cripto*-null mutants, was expressed in the posterior region of *cripto*$^{F78A/F78A}$ embryos (Fig. S1, C and C′). These results demonstrate that *cripto*$^{F78A/F78A}$ homozygotes establish an A–P axis and arrest development at a later stage compared with null mutants.

To characterize gastrulation defects in *cripto*$^{F78A/F78A}$ mutant embryos, we next visualized derivatives of the anterior primitive streak, such as the node, a structure that expresses *Nodal* and *Foxa2*, and the axial mesoderm or anterior definitive endoderm, which are marked by *Foxa2*, *Chordin*, or *Cer-1* mRNAs (Fig. 3, B–E; Monaghan et al., 1993; Conlon et al., 1994; Biben et al., 1998; Bachiller et al., 2000). In *cripto*-null mutants, expression of *Foxa2* was absent and *Nodal* expression was confined to the proximal epiblast, confirming that node formation is inhibited (Fig. 3 B″). In *cripto*$^{F78A/F78A}$ mutants, *Nodal* and *Foxa2* expression were clearly detected in the distal tip of the rudimentary

primitive streak, suggesting that anterior primitive streak derivatives are specified (Fig. 3, B′ and C′). Moreover, *Foxa2* mRNA staining revealed that axial mesendoderm populations are also present more anteriorly (Fig. 3 C′, s1), whereas they are missing in *cripto*-null mutants (Fig. 3 C′′). Similarly, *Cer-1* was clearly induced in 5 out of 10 *cripto*$^{F78A/F78A}$ mutants, even though the mRNA level was reduced and its expression domain extended to more posterior regions compared with wild-type controls (Fig. 3, D and D′). Likewise, *Chordin* was undetectable in *cripto*-null embryos but expressed in 3 out of 10 of the *cripto*$^{F78A/F78A}$ mutants that were analyzed (Fig. 3, E and E′ [arrowhead]). Thus, compared with a *cripto*-null mutation, the F78A substitution has only relatively mild inhibitory effects on mesendoderm and primitive streak formation.

Nodal signaling is impaired in cripto$^{F78A/F78A}$ embryos

Several studies in mice, *X. laevis*, and zebrafish link Cripto to the Nodal pathway (Shen and Schier, 2000). Therefore, to assess the role of residue F78 of Cripto, we analyzed the expression pattern of *Nodal* and its target genes, *Lefty1* and *2*, in *cripto*$^{F78A/F78A}$ and *cripto*-null mutants at 6.75 dpc. At this stage, *Nodal* is expressed throughout the primitive streak and posterior mesoderm in wild-type embryos (Fig. 4 A; Conlon et al., 1994; Collignon et al., 1996). In contrast, in both *cripto*$^{F78A/F78A}$ and *cripto*-null mutants, *Nodal* expression was reduced and remained at the rim of the proximal epiblast (Fig. 4, A′ and A′′). Next, to assess whether Nodal signaling was induced, we analyzed the expression of *Lefty1* and *2*. In wild-type embryos at 6.75 dpc, *Lefty1* is expressed in the anterior visceral endoderm, whereas *Lefty2* marks the nascent mesoderm generated from the primitive streak (Fig. 4 B; Meno et al., 1997). Expression of both *Lefty1* and *2* was absent in *cripto*-null mutants (Fig. 4 B′′). Interestingly, both genes were induced in *cripto*$^{F78A/F78A}$ embryos, although below normal levels (Fig. 4 B′). To determine whether Nodal signaling is also maintained at later stages in *cripto*$^{F78A/F78A}$ embryos, we analyzed the expression pattern of *Lefty2*, a direct *Nodal* target gene, and *Fgf8* at 7.5 dpc. As expected, both genes were readily detectable in the primitive streak of wild-type embryos (Fig. 4 C) but not in *cripto*-null mutants (Fig. 4 C′′). In contrast, *Lefty2* mRNA was detected in a subset of cells in the posterior side of *cripto*$^{F78A/F78A}$ embryos (Fig. 4 C′). Furthermore, *Fgf8* was expressed in *cripto*$^{F78A/F78A}$ mutants and its expression domain was even enlarged and extended into the extraembryonic region (Fig. 4 C′). Collectively, these data strongly suggest that the strength or duration of Nodal signaling in *cripto*$^{F78A/F78A}$ embryos is perturbed compared with wild-type embryos, although it significantly exceeds that observed in *cripto*-null mutants.

Cripto^{F78A} fails to potentiate Nodal signaling in cell culture but retains MAPK activity

Previous analysis of ES cell–derived EBs suggested that F78 is essential for Cripto to stimulate the in vitro differentiation of cardiomyocytes (Parisi et al., 2003). Similarly, substitution of F78 by alanine entirely blocks the ability of Cripto to rescue

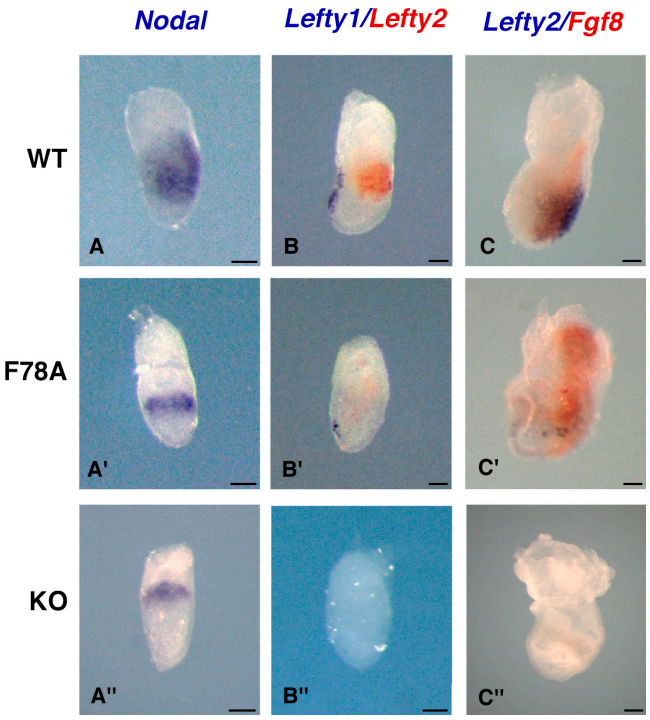

Figure 4. **Effector genes in the Nodal pathway are only partially inhibited in *cripto*$^{F78A/F78A}$ mutants.** (A, A′, and A′′) Wild-type (top), *cripto*$^{F78A/F78A}$ (middle), and *cripto*-null (bottom) embryos stained for *Nodal* at 6.75 dpc. In the wild type, *Nodal* marks the primitive streak and the posterior mesoderm (A), whereas it is confined to the rim of the proximal epiblast in both *cripto*$^{F78A/F78A}$ (A′) and *cripto*-null embryos (A′′). (B, B′, and B′′) Expression of *Lefty1* (blue) and *2* (red) mRNA at 6.75 dpc. In the wild type, *Lefty1* marks the anterior visceral endoderm, whereas *Lefty2* is expressed in the nascent mesoderm (B). *Lefty1* and *2* are weakly expressed in *cripto*$^{F78A/F78A}$ embryos (B′) but are completely absent in *cripto*-null mutants (B′′). (C, C′, and C′′) At 7.5 dpc, wild-type embryos express both *Lefty2* (blue) and *Fgf8* (red) in the primitive streak (C). In *cripto*$^{F78A/F78A}$ embryos, *Lefty2* expression is detectable at reduced levels at the posterior pole of the embryo. Conversely, *Fgf8* expression is up-regulated and ectopically extends into the extraembryonic region (C′). In sharp contrast, *cripto*-null mutants express neither *Lefty2* nor *Fgf8* (C′′). Bars, 50 µm.

gastrulation of *oep* mutant zebrafish embryos (Minchiotti et al., 2001). Given these reports, it was surprising that substitution of F78 by alanine only partially inhibited Cripto activity in the mouse embryo. To determine whether Cripto^{F78A} can stimulate Nodal signaling in cell culture, we monitored its effect on CAGA-luc, a well characterized and sensitive luciferase reporter of ALK4–Smad3 signaling. Although transfection of wild-type *cripto* potently stimulated the activity of Nodal, Cripto^{F78A} was completely inactive in this assay (Fig. 5 A). Analogous results were obtained using the activin response element (ARE)–luc reporter construct in conjunction with wild-type Nodal or a more potent supercleaved and stabilized derivative (Nsc-g; Fig. S2, available at http://www.jcb.org/cgi/content/full/jcb.200709090/DC1; Yan et al., 2002; Le Good et al., 2005; Chen et al., 2006; Andersson et al., 2007). These results suggest that Cripto^{F78A} is unable to activate a Nodal–ALK4–Smad signaling complex.

Cripto can also potentiate growth/differentiation factor (GDF) 1 and 3 signaling (Andersson et al., 2007), raising the question of whether these activities rely on F78 in a manner

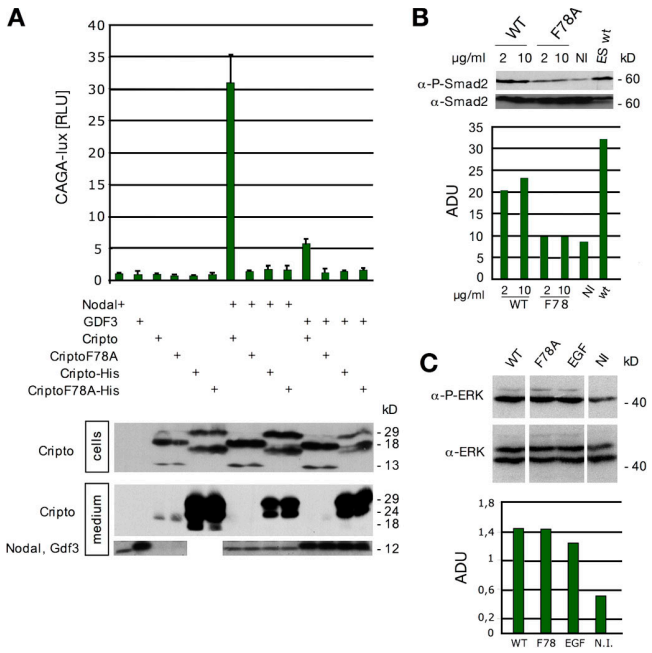

Figure 5. **Cripto^{F78A} does not support the activation of Smad2,3 by Nodal or GDF3 in cell-based assays.** (A) Upon transfection in 293T cells, wild-type Cripto potentiates Nodal and GDF3 activity in a Smad3-dependent luciferase assay, whereas the F78A mutant is inactive. 293T cells were transfected with the luciferase reporter CAGA-Luc. The plasmids encoding native ligands, either GDF3 or Nodal, were transfected with or without wild-type or F78A Cripto or secreted Cripto-His constructs. Experiments were performed in triplicate. The expression of input proteins, as detected by Western blotting, is shown at the bottom. Secreted forms of wild-type and F78A Cripto lacking the GPI anchor were inactive in this assay. Error bars represent SD of three experiments. RLU, relative luciferase unit. (B) Wild-type, but not F78A, Cripto activates Smad2 in ES cells. 2-d-old *Cripto*$^{-/-}$ EBs were serum starved for 3 h and then treated with either wild-type or F78A recombinant Cripto protein for 20 min or left untreated (NI) as indicated. Wild-type ES cell–derived EBs were used as a control. Smad2 activation was detected by Western blot analysis using anti–phospho-Smad2 antibody. Levels of total Smad2 were also compared. Densitometry analyses were performed using the ImageQuant 5.2 software (GE Healthcare). Smad2 phosphorylation was expressed as the ratio between arbitrary densitometric units (ADU) of P-Smad2 and total Smad2. (C) F78A recombinant Cripto retains its ability to activate phospho-ERK. Serum-starved *Cripto*$^{-/-}$ EBs were treated with 2 µg/ml of either wild-type or F78A recombinant Cripto protein for 10 min or left untreated (NI) as indicated. ERK activation was detected by Western blot analysis using anti–phospho-ERK antibody. Densitometry analyses were performed as in B.

similar to Nodal. Unlike wild-type Cripto, the Cripto^{F78A} mutant failed to potentiate GDF1 or 3 signaling in this assay (Fig. 5 A and not depicted).

Cripto^{F78A} might activate the Smad2 pathway only in an embryo-like cell context. To test this, 2-d-old *Cripto*$^{-/-}$ ES cell–derived EBs were starved in low serum for 3 h and then stimulated with recombinant soluble Cripto or the F78A mutant protein. Consistent with published data (Watanabe et al., 2007), Cripto without a GPI anchor was poorly active but, when applied at elevated concentrations, it significantly increased the phosphorylation of Smad2 (Fig. 5 B). In contrast, soluble Cripto^{F78A} failed to detectably stimulate Smad2 phosphorylation (Fig. 5 B). However, mutation of F78 did not diminish the ability of Cripto to stimulate the MAPK signaling pathway (Fig. 5 C). Thus, we conclude that the F78A mutation selectively impairs Nodal–ALK4–Smad2,3 while leaving intact Smad-independent signals mediated by MAPK.

Discussion

Cripto$^{F78A/F78A}$ embryos establish an A–P axis and initiate gastrulation

Understanding how Cripto stimulates Nodal-dependent cell movements in the visceral endoderm and epiblast is fundamental to our understanding of how the A–P body axis is established in mammalian embryos. In *cripto*$^{-/-}$ embryos, distal visceral endoderm do not move, and the vast majority of cells in the epiblast adopt a neuroectodermal character because mesendoderm progenitors, which form the primitive streak, are either absent or remain confined to the proximal epiblast (Ding et al., 1998; Liguori et al., 2003). In this paper, we show that homozygous mutants carrying the novel *cripto*^{F78A} allele display less severe defects than *cripto*$^{-/-}$ embryos. In particular, definitive endoderm and axial mesoderm populations marked by *Cer-1* and *Foxa2* transcripts are readily detectable, and neural progenitors expressing *Otx2* mRNA consistently localize to the anterior region. In some instances, anterior-most midline cells also express the axial marker *Chordin*, which is consistent with their mesendodermal origin. Likewise, posterior cells expressing *Fgf8* and *Brachyury* that are absent or immobilised in the proximal epiblast of *cripto*-null embryos (Ding et al., 1998) clearly ingress in the primitive streak of *cripto*$^{F78A/F78A}$ mutants, even though this structure remains abnormally short and eventually fails to form a morphologically distinguishable node or notochord. Thus, in sharp contrast to *cripto*-null mutants, *cripto*$^{F78A/F78A}$ embryos establish an A–P axis and initiate gastrulation, suggesting that this mutant allele encodes a functional hypomorph.

The phenotype of *cripto*$^{F78A/F78A}$ embryos is reminiscent of patterning defects that arise when Nodal autoinduction is inhibited (Hoodless et al., 2001; Yamamoto et al., 2001; Norris et al., 2002). During normal development, *Nodal* expression is initiated in the proximal epiblast and, upon activation of an autoregulatory enhancer by FoxH1, spreads to the visceral endoderm and distal epiblast (Brennan et al., 2001; Norris et al., 2002). In this paper, we show that both *cripto*$^{F78A/F78A}$ and *cripto*-null mutants fail to expand the Nodal expression domain, confirming that Smad-dependent autoinductive Nodal signaling is inhibited. However, interestingly, mutant Cripto^{F78A} protein was sufficient to induce or prolong the expression of several other Nodal target genes, including *Lefty1*, *Lefty2*, and *Fgf8*, which were completely silenced in *cripto*-null mutants at the stages examined.

These results substantiate our conclusion that *cripto*^{F78A} is a hypomorphic allele that is sufficient to mediate Alk4–Smad–FoxH1–indpendent Nodal signaling. They can also explain why primitive streak and posterior mesoderm formation are relatively mildly perturbed in *cripto*$^{F78A/F78A}$ mutants, because previous analysis of *FoxH1* mutants (Hoodless et al., 2001; Yamamoto et al., 2001) and hypomorphic alleles of *Nodal* (Lowe et al., 2001; Norris et al., 2002; Vincent et al., 2003; Ben-Haim et al., 2006) established that posterior mesoderm formation requires lower levels of Nodal signaling compared with axial midline structures.

Cripto^{F78A} fails to potentiate Nodal signaling

Previous studies have shown that Cripto strictly depends on residue F78 to rescue mutant zebrafish embryos lacking the Nodal coreceptor oep. Using cell-based activity assays, we confirmed in this paper that Cripto^{F78A} protein fails to stimulate well-characterized Nodal luciferase reporter genes, which specifically rely on ALK4–Smad–FoxH1 signaling. Furthermore, Cripto^{F78A} is also unable to significantly activate Smad2 in ES cell–derived EBs, a model that more closely mimics a physiological environment. Coimmunoprecipitation experiments in transfected cells previously established that Cripto can directly bind both Nodal and ALK4 to potentiate Nodal signaling (Reissmann et al., 2001; Yeo and Whitman, 2001). However, a triple mutant of the EGF-like domain comprising the F78 residue completely abolished the ability of Cripto to stimulate the induction of a Nodal luciferase reporter in mammalian tissue culture cells (Yan et al., 2002). Moreover, chemical cross-linking experiments in 293T cells, followed by coimmunoprecipitation, suggest that this triple mutant fails to bind Nodal, whereas it interacts with the ALK4 receptor in a manner similar to that of the wild type (Yan et al., 2002). The present results are thus consistent with a model in which the F78 residue of Cripto is essential to assemble functional Cripto–ALK4 receptor complexes and thereby potentiate a Nodal autoregulatory feedback loop.

Luciferase reporter assays and coimmunoprecipitation experiments suggest that Cripto can also potentiate Nodal signaling through ALK7 (Reissmann et al., 2001). Therefore, it is formally possible that the loss of F78 selectively blocks the ability of Cripto to activate ALK4 without affecting Nodal signaling via the ALK7 receptor. However, it has previously been shown that ALK7 is dispensable and unable to compensate for the loss of ALK4 in the mouse embryo (Gu et al., 1998; Jornvall et al., 2004). Cripto can also stimulate the induction of CAGA-luc reporter by native forms of GDF1 and 3 (Andersson et al., 2007). In contrast, as observed with Nodal, GDF1 and 3 failed to signal through Cripto^{F78A}. However, our data do not rule out the possibility that F78 may retain the ability to influence Smad signaling by other ligands, including activins or TGF-β.

Cripto can also regulate several Smad-independent signals in various biological contexts (Adamson et al., 2002; Strizzi et al., 2005). Our results show that Cripto^{F78A} retains the ability to activate MAPK in embryo bodies, which may contribute to the residual activity of Cripto^{F78A} observed in vivo. In keeping with this idea, Cripto also stimulates MAPK–AKT phosphorylation in mouse mammary epithelial cells independently of Nodal and ALK4 (Bianco et al., 2002), possibly through the association with the membrane-associated heparan sulfate proteoglycan glypican 1 (Bianco et al., 2003), and overexpression of *cripto* in mammary epithelial cells promotes epithelial-mesenchymal transitions and cell motility through a MAPK-dependent pathway (Strizzi et al. 2005). In contrast, *cripto* and its putative homologue FRL-1 have recently also been shown to bind Wnt11 and stimulate the canonical Wnt–β-catenin–Lef-1 signaling pathway in *X. laevis* (Tao et al., 2005). Finally, it is worth noting that recent data highlight a novel role of Cripto as a TGF-β antagonist and propose that Cripto antagonism of TGF-β signaling may contribute to tumor initiation and progression (Gray et al., 2006).

Based on this consideration, we believe that genetic manipulations, which selectively inhibit a subset of signaling activities, will be crucial to unambiguously dissect the complex functions of Cripto in vivo. Accordingly, our data provide the first in vivo evidence that Cripto initiates gastrulation movements independently of its known stimulatory effect on the canonical Nodal–ALK4–Smad2 signaling and open the way to dissect the complex network of Cripto signaling in vivo. It will be important to determine, in future studies, whether Nodal–ALK4–Smad–independent Cripto activities in vivo are mediated by the Wnt pathway, MAPK, or possibly other signaling pathways.

Materials and methods

Targeting of the cripto locus

The targeting vector was derived from pFlox vector (Chen et al., 1998) by excision of a SmaI–BamHI DNA fragment spanning the loxP site and by removing the BglI–SmaI DNA fragment spanning the *hsv-tk* gene (Fig.1 A). A 3.5-kb 5′ homologous sequence spanning exons 1 and 2 was inserted upstream of the loxP site–flanked cassette encoding the *neo*^{r} gene. A 5.6-kb 3′ homologous sequence spanning exons 3 to 6 was inserted downstream of the *neo*^{r} gene (Fig. 1 A). The two overlapping PCR primers 5′F78A (5′-GCATCCTGGGGTCCGCCTGTGCCTGCCCTC-3′) and 3′F78A (5′-GGAGGGCAGGCACAGGCGGACCCCAGGATGC-3′) were used to introduce the F78A point mutation in the targeting vector (underlining in primers indicates the nucleotide sequence that was modified to insert the F78A mutation).

RI ES cells were transfected with the targeting vector and selected in G-418. DNA prepared from individual drug-resistant colonies was digested with EcoRV for Southern blot analysis using a 600-bp 5′ external probe (RH5 in Fig.1 [A and B]), a 500-bp 3′ internal probe (BE6 in Fig. 1 [A and B]), and a neo^r probe. After identification of the targeted clones, the presence of the point mutation was verified by PCR amplification and sequence analysis. Selected ES cell lines were used to generate germline chimeric mice that were subsequently bred to C57BL/6 females (Charles River Laboratories). F1 *cripto*^{F78Aneo} heterozygotes were crossed with a *pgk-Cre* deletion strain.

Mouse breeding and genotyping

Heterozygous mice for the *cripto*^{F78A} allele were maintained on a mixed genetic background C57BL/6 × Sv129. Heterozygous mice for the *cripto*-null allele were maintained on a mixed genetic background (C57BL/6 × Sv129 × Black Swiss) and also backcrossed to an inbred C57BL/6 strain. No phenotypic differences were observed between *cripto*-null embryos on different genetic backgrounds. Timed matings between heterozygotes were used to obtain both *cripto*$^{F78A/F78A}$ and *cripto*-null homozygous mutant embryos. Embryos were genotyped by PCR at 7.5 dpc using extraembryonic tissues. At 6.75 dpc, DNA was extracted from whole embryos for genotyping.

Whole mount immunohistochemistry and in situ hybridization

Embryos were dissected in PBS and fixed in 4% paraformaldehyde in PBS at 4°C for 2–16 h, washed in PBT (0.1% Tween 20 in PBS), dehydrated through graded methanol, and stored in 100% methanol at −20°C. For immunohistochemistry, embryos were rehydrated in PBTx (0.25% Triton X-100 in PBS), bleached with 0.05% H_2O_2 overnight, blocked with PBTsb (10% normal goat serum and 1 mg/ml BSA in PBTx), and incubated overnight at 4°C with 2 μg/ml of affinity-purified α-Cripto antibodies. To remove the unbound antibody, embryos were extensively washed in PBTx (1 h, six times) and labeled with biotinylated secondary antibody overnight at 4°C. After six washes in PBTx, embryos were incubated with biotin–streptavidin complex (AB complex; Vector Laboratories), revealed by incubation for 30 min with 0.5 mg/ml of 3–3′ diaminobenzidine (Sigma-Aldrich), and developed by addition of 0.03% H_2O_2. Stained embryos were examined and photographed using a stereomicroscope (MZ12; Leica). All images were processed in Photoshop 5.0 (Adobe).

Whole mount immunohistochemistry and in situ hybridization was performed according to standard procedures (Liguori et al., 2003). Probes for the following genes were used in this study: *Brachyury* (Wilkinson et al., 1990), *Cerberus-like* (Belo et al., 1997), *Chordin* (Bachiller et al., 2000),

Fgf8 (Crossley and Martin, 1995), *Foxa2* (Monaghan et al., 1993), *Krox20* (Wilkinson et al., 1989), *Lefty1* and *2* (Meno et al., 1996; Branford and Yost, 2002), *Mox1* (Candia et al., 1992), *Nodal* (Varlet et al., 1997), and *Otx2* (Acampora et al., 1995). J.A. Belo (Istituto Gulbenkian de Ciencia, Oeiras, Portugal), K. Chien (Harvard University, Cambridge, MA), R. Di Lauro (Università Federico II, Napoli, Italy), S. Filosa (Institute of Genetics and Biophysics "A. Buzzati-Traverso," Naples, Italy), H. Hamada (Osaka University, Osaka, Japan), A. Simeone (Ceinge, Naples, Italy), and M. Studer (Telethon Institute of Genetics and Medicine, Naples, Italy) provided plasmids.

Cripto activity assay in transiently transfected 293T cells

Cripto activity assays were performed as previously described (Yan et al., 2002; Andersson et al., 2007) by transiently transfecting 293T cells with either the ARE-luc or the pCAGA-luc luciferase reporter constructs and expression vectors for Cripto, FoxH1, and wild type or a stabilized form of Nodal (Nsc-g; Le Good et al., 2005).

ES cell differentiation assay and Western blot

The ES cell lines RI and *cripto*$^{-/-}$ DE7 were used throughout the study and differentiation assays were performed as previously described (Parisi et al., 2003). Western blot analysis was performed as previously described (Parisi et al., 2003). Anti–phospho-Smad2 (Ser465/467), total Smad2 (Cell Signaling Technology), and anti–phospho–extracellular signal–regulated kinase (ERK; Santa Cruz Biotechnology, Inc.) antibodies were used according to the manufacturer's instructions.

Online supplemental material

Fig. S1 contains additional information on the embryonic development of *cripto*$^{F78A/F78A}$ mutants at the head-fold stage. Fig. S2 contains additional information on Cripto activity in the 293 cell ARE-luc reporter assay and shows that F78A mutant is inactive in this assay. Online supplemental material is available at http://www.jcb.org/cgi/content/full/jcb.200709090/DC1.

We thank Mrs. M. Terracciano for technical assistance and Raffaele Improta and Ivan Solombrino for animal care. The Biogem transgenic facility is acknowledged for technical assistance in generating targeted ES cells and chimeric mice. J.A. Belo, K. Chien, R. Di Lauro, S. Filosa, H. Hamada, Y. Saga, A. Simeone, and M. Studer are acknowledged for their kind gifts of plasmids. We thank Anna Aliperti for proofreading the manuscript.

This work was supported by grants from the Associazione Italiana Ricerca sul Cancro to M.G. Persico and G. Minchiotti and from the Fondo per gli Investimenti della Ricerca di Base to M.G. Persico. D. D'Andrea was supported by a fellowship from the Fondazione Italiana Ricerca sul Cancro.

Submitted: 14 September 2007
Accepted: 9 January 2008

References

Acampora, D., S. Mazan, Y. Lallemand, V. Avantaggiato, M. Maury, A. Simeone, and P. Brulet. 1995. Forebrain and midbrain regions are deleted in Otx2−/− mutants due to a defective anterior neuroectoderm specification during gastrulation. *Development.* 121:3279–3290.

Adamson, E.D., G. Minchiotti, and D.S. Salomon. 2002. Cripto: a tumor growth factor and more. *J. Cell. Physiol.* 190:267–278.

Adkins, H.B., C. Bianco, S.G. Schiffer, P. Rayhorn, M. Zafari, A.E. Cheung, O. Orozco, D. Olson, A. De Luca, L.L. Chen, et al. 2003. Antibody blockade of the Cripto CFC domain suppresses tumor cell growth in vivo. *J. Clin. Invest.* 112:575–587.

Andersson, O., P. Bertolino, and C.F. Ibanez. 2007. Distinct and cooperative roles of mammalian Vg1 homologs GDF1 and GDF3 during early embryonic development. *Dev. Biol.* 311:500–511.

Bachiller, D., J. Klingensmith, C. Kemp, J.A. Belo, R.M. Anderson, S.R. May, J.A. McMahon, A.P. McMahon, R.M. Harland, J. Rossant, and E.M. De Robertis. 2000. The organizer factors Chordin and Noggin are required for mouse forebrain development. *Nature.* 403:658–661.

Baldassarre, G., A. Romano, F. Armenante, M. Rambaldi, I. Paoletti, C. Sandomenico, S. Pepe, S. Staibano, G. Salvatore, G. De Rosa, et al. 1997. Expression of teratocarcinoma-derived growth factor-1 (TDGF-1) in testis germ cell tumors and its effects on growth and differentiation of embryonal carcinoma cell line NTERA2/D1. *Oncogene.* 15:927–936.

Belo, J.A., T. Bouwmeester, L. Leyns, N. Kertesz, M. Gallo, M. Follettie, and E.M. De Robertis. 1997. Cerberus-like is a secreted factor with neutralizing activity expressed in the anterior primitive endoderm of the mouse gastrula. *Mech. Dev.* 68:45–57.

Ben-Haim, N., C. Lu, M. Guzman-Ayala, L. Pescatore, D. Mesnard, M. Bischofberger, F. Naef, E.J. Robertson, and D.B. Constam. 2006. The nodal precursor acting via activin receptors induces mesoderm by maintaining a source of its convertases and BMP4. *Dev. Cell.* 11:313–323.

Bianco, C., H.B. Adkins, C. Wechselberger, M. Seno, N. Normanno, A. De Luca, Y. Sun, N. Khan, N. Kenney, A. Ebert, et al. 2002. Cripto-1 activates nodal- and ALK4-dependent and -independent signaling pathways in mammary epithelial Cells. *Mol. Cell. Biol.* 22:2586–2597.

Bianco, C., L. Strizzi, A. Rehman, N. Normanno, C. Wechselberger, Y. Sun, N. Khan, M. Hirota, H. Adkins, K. Williams, et al. 2003. A Nodal- and ALK4-independent signaling pathway activated by Cripto-1 through Glypican-1 and c-Src. *Cancer Res.* 63:1192–1197.

Biben, C., E. Stanley, L. Fabri, S. Kotecha, M. Rhinn, C. Drinkwater, M. Lah, C.C. Wang, A. Nash, D. Hilton, et al. 1998. Murine cerberus homologue mCer-1: a candidate anterior patterning molecule. *Dev. Biol.* 194:135–151.

Branford, W.W., and H.J. Yost. 2002. Lefty-dependent inhibition of Nodal- and Wnt-responsive organizer gene expression is essential for normal gastrulation. *Curr. Biol.* 12:2136–2141.

Brennan, J., C.C. Lu, D.P. Norris, T.A. Rodriguez, R.S. Beddington, and E.J. Robertson. 2001. Nodal signalling in the epiblast patterns the early mouse embryo. *Nature.* 411:965–969.

Candia, A.F., J. Hu, J. Crosby, P.A. Lalley, D. Noden, J.H. Nadeau, and C.V. Wright. 1992. Mox-1 and Mox-2 define a novel homeobox gene subfamily and are differentially expressed during early mesodermal patterning in mouse embryos. *Development.* 116:1123–1136.

Chen, C., and M.M. Shen. 2004. Two modes by which Lefty proteins inhibit nodal signaling. *Curr. Biol.* 14:618–624.

Chen, C., S.M. Ware, A. Sato, D.E. Houston-Hawkins, R. Habas, M.M. Matzuk, M.M. Shen, and C.W. Brown. 2006. The Vg1-related protein Gdf3 acts in a Nodal signaling pathway in the pre-gastrulation mouse embryo. *Development.* 133:319–329.

Chen, J., S.W. Kubalak, and K.R. Chien. 1998. Ventricular muscle-restricted targeting of the RXRalpha gene reveals a non-cell-autonomous requirement in cardiac chamber morphogenesis. *Development.* 125:1943–1949.

Cheng, S.K., F. Olale, J.T. Bennett, A.H. Brivanlou, and A.F. Schier. 2003. EGF-CFC proteins are essential coreceptors for the TGF-beta signals Vg1 and GDF1. *Genes Dev.* 17:31–36.

Ciardiello, F., R. Dono, N. Kim, M.G. Persico, and D.S. Salomon. 1991. Expression of cripto, a novel gene of the epidermal growth factor gene family, leads to in vitro transformation of a normal mouse mammary epithelial cell line. *Cancer Res.* 51:1051–1054.

Ciccodicola, A., R. Dono, S. Obici, A. Simeone, M. Zollo, and M.G. Persico. 1989. Molecular characterization of a gene of the 'EGF family' expressed in undifferentiated human NTERA2 teratocarcinoma cells. *EMBO J.* 8:1987–1991.

Colas, J.F., and G.C. Schoenwolf. 2000. Subtractive hybridization identifies chick-cripto, a novel EGF-CFC ortholog expressed during gastrulation, neurulation and early cardiogenesis. *Gene.* 255:205–217.

Collignon, J., I. Varlet, and E.J. Robertson. 1996. Relationship between asymmetric nodal expression and the direction of embryonic turning. *Nature.* 381:155–158.

Conlon, F.L., K.M. Lyons, N. Takaesu, K.S. Barth, A. Kispert, B. Herrmann, and E.J. Robertson. 1994. A primary requirement for nodal in the formation and maintenance of the primitive streak in the mouse. *Development.* 120:1919–1928.

Crossley, P.H., and G.R. Martin. 1995. The mouse Fgf8 gene encodes a family of polypeptides and is expressed in regions that direct outgrowth and patterning in the developing embryo. *Development.* 121:439–451.

Ding, J., L. Yang, Y.T. Yan, A. Chen, N. Desai, A. Wynshaw-Boris, and M.M. Shen. 1998. Cripto is required for correct orientation of the anterior-posterior axis in the mouse embryo. *Nature.* 395:702–707.

Dono, R., L. Scalera, F. Pacifico, D. Acampora, M.G. Persico, and A. Simeone. 1993. The murine cripto gene: expression during mesoderm induction and early heart morphogenesis. *Development.* 118:1157–1168.

Dorey, K., and C.S. Hill. 2006. A novel Cripto-related protein reveals an essential role for EGF-CFCs in Nodal signalling in *Xenopus* embryos. *Dev. Biol.* 292:303–316.

Gray, P.C., C.A. Harrison, and W. Vale. 2003. Cripto forms a complex with activin and type II activin receptors and can block activin signaling. *Proc. Natl. Acad. Sci. USA.* 100:5193–5198.

Gray, P.C., G. Shani, K. Aung, J. Kelber, and W. Vale. 2006. Cripto binds transforming growth factor beta (TGF-beta) and inhibits TGF-beta signaling. *Mol. Cell. Biol.* 26:9268–9278.

Gu, Z., M. Nomura, B.B. Simpson, H. Lei, A. Feijen, J. van den Eijnden-van Raaij, P.K. Donahoe, and E. Li. 1998. The type I activin receptor ActRIB is required for egg cylinder organization and gastrulation in the mouse. *Genes Dev.* 12:844–857.

Harms, P.W., and C. Chang. 2003. Tomoregulin-1 (TMEFF1) inhibits nodal signaling through direct binding to the nodal coreceptor Cripto. *Genes Dev.* 17:2624–2629.

Harrison, C.A., P.C. Gray, W.W. Vale, and D.M. Robertson. 2005. Antagonists of activin signaling: mechanisms and potential biological applications. *Trends Endocrinol. Metab.* 16:73–78.

Hoodless, P.A., M. Pye, C. Chazaud, E. Labbe, L. Attisano, J. Rossant, and J.L. Wrana. 2001. FoxH1 (Fast) functions to specify the anterior primitive streak in the mouse. *Genes Dev.* 15:1257–1271.

Jornvall, H., E. Reissmann, O. Andersson, M. Mehrkash, and C.F. Ibanez. 2004. ALK7, a receptor for nodal, is dispensable for embryogenesis and left-right patterning in the mouse. *Mol. Cell. Biol.* 24:9383–9389.

Kinoshita, N., J. Minshull, and M.W. Kirschner. 1995. The identification of two novel ligands of the FGF receptor by a yeast screening method and their activity in *Xenopus* development. *Cell.* 83:621–630.

Le Good, J.A., K. Joubin, A.J. Giraldez, N. Ben-Haim, S. Beck, Y. Chen, A.F. Schier, and D.B. Constam. 2005. Nodal stability determines signaling range. *Curr. Biol.* 15:31–36.

Liguori, G.L., D. Echevarria, R. Improta, M. Signore, E. Adamson, S. Martinez, and M.G. Persico. 2003. Anterior neural plate regionalization in cripto null mutant mouse embryos in the absence of node and primitive streak. *Dev. Biol.* 264:537–549.

Lowe, L.A., S. Yamada, and M.R. Kuehn. 2001. Genetic dissection of nodal function in patterning the mouse embryo. *Development.* 128:1831–1843.

Massague, J., and Y.G. Chen. 2000. Controlling TGF-beta signaling. *Genes Dev.* 14:627–644.

Meno, C., Y. Saijoh, H. Fujii, M. Ikeda, T. Yokoyama, M. Yokoyama, Y. Toyoda, and H. Hamada. 1996. Left-right asymmetric expression of the TGF beta-family member lefty in mouse embryos. *Nature.* 381:151–155.

Meno, C., Y. Ito, Y. Saijoh, Y. Matsuda, K. Tashiro, S. Kuhara, and H. Hamada. 1997. Two closely-related left-right asymmetrically expressed genes, lefty-1 and lefty-2: their distinct expression domains, chromosomal linkage and direct neuralizing activity in *Xenopus* embryos. *Genes Cells.* 2:513–524.

Minchiotti, G., G. Manco, S. Parisi, C.T. Lago, F. Rosa, and M.G. Persico. 2001. Structure-function analysis of the EGF-CFC family member Cripto identifies residues essential for nodal signalling. *Development.* 128:4501–4510.

Monaghan, A.P., K.H. Kaestner, E. Grau, and G. Schutz. 1993. Postimplantation expression patterns indicate a role for the mouse forkhead/HNF-3 alpha, beta and gamma genes in determination of the definitive endoderm, chordamesoderm and neuroectoderm. *Development.* 119:567–578.

Norris, D.P., J. Brennan, E.K. Bikoff, and E.J. Robertson. 2002. The Foxh1-dependent autoregulatory enhancer controls the level of Nodal signals in the mouse embryo. *Development.* 129:3455–3468.

Onuma, Y., C.Y. Yeo, and M. Whitman. 2006. XCR2, one of three *Xenopus* EGF-CFC genes, has a distinct role in the regulation of left-right patterning. *Development.* 133:237–250.

Parisi, S., D. D'Andrea, C.T. Lago, E.D. Adamson, M.G. Persico, and G. Minchiotti. 2003. Nodal-dependent Cripto signaling promotes cardiomyogenesis and redirects the neural fate of embryonic stem cells. *J. Cell Biol.* 163:303–314.

Reissmann, E., H. Jornvall, A. Blokzijl, O. Andersson, C. Chang, G. Minchiotti, M.G. Persico, C.F. Ibanez, and A.H. Brivanlou. 2001. The orphan receptor ALK7 and the Activin receptor ALK4 mediate signaling by Nodal proteins during vertebrate development. *Genes Dev.* 15:2010–2022.

Sakuma, R., Y. Ohnishi Yi, C. Meno, H. Fujii, H. Juan, J. Takeuchi, T. Ogura, E. Li, K. Miyazono, and H. Hamada. 2002. Inhibition of Nodal signalling by Lefty mediated through interaction with common receptors and efficient diffusion. *Genes Cells.* 7:401–412.

Salomon, D.S., C. Bianco, and M. De Santis. 1999. Cripto: a novel epidermal growth factor (EGF)-related peptide in mammary gland development and neoplasia. *Bioessays.* 21:61–70.

Schiffer, S.G., S. Foley, A. Kaffashan, X. Hronowski, A.E. Zichittella, C.Y. Yeo, K. Miatkowski, H.B. Adkins, B. Damon, M. Whitman, et al. 2001. Fucosylation of Cripto is required for its ability to facilitate nodal signaling. *J. Biol. Chem.* 276:37769–37778.

Shen, M.M., and A.F. Schier. 2000. The EGF-CFC gene family in vertebrate development. *Trends Genet.* 16:303–309.

Shen, M.M., H. Wang, and P. Leder. 1997. A differential display strategy identifies Cryptic, a novel EGF-related gene expressed in the axial and lateral mesoderm during mouse gastrulation. *Development.* 124:429–442.

Shi, S., C. Ge, Y. Luo, X. Hou, R.S. Haltiwanger, and P. Stanley. 2007. The threonine that carries fucose, but not fucose, is required for Cripto to facilitate Nodal signaling. *J. Biol. Chem.* 282:20133–20141.

Simeone, A., D. Acampora, A. Mallamaci, A. Stornaiuolo, M.R. D'Apice, V. Nigro, and E. Boncinelli. 1993. A vertebrate gene related to orthodenticle contains a homeodomain of the bicoid class and demarcates anterior neuroectoderm in the gastrulating mouse embryo. *EMBO J.* 12:2735–2747.

Strizzi, L., C. Bianco, N. Normanno, and D. Salomon. 2005. Cripto-1: a multifunctional modulator during embryogenesis and oncogenesis. *Oncogene.* 24:5731–5741.

Tao, Q., C. Yokota, H. Puck, M. Kofron, B. Birsoy, D. Yan, M. Asashima, C.C. Wylie, X. Lin, and J. Heasman. 2005. Maternal wnt11 activates the canonical wnt signaling pathway required for axis formation in *Xenopus* embryos. *Cell.* 120:857–871.

Varlet, I., J. Collignon, and E.J. Robertson. 1997. nodal expression in the primitive endoderm is required for specification of the anterior axis during mouse gastrulation. *Development.* 124:1033–1044.

Vincent, S.D., N.R. Dunn, S. Hayashi, D.P. Norris, and E.J. Robertson. 2003. Cell fate decisions within the mouse organizer are governed by graded Nodal signals. *Genes Dev.* 17:1646–1662.

Watanabe, K., S. Hamada, C. Bianco, M. Mancino, T. Nagaoka, M. Gonzales, V. Bailly, L. Strizzi, and D.S. Salomon. 2007. Requirement of glycosylphosphatidylinositol anchor of cripto-1 for 'trans' activity as a nodal co-receptor. *J. Biol. Chem.* 282:35772–35786.

Wilkinson, D.G., S. Bhatt, P. Chavrier, R. Bravo, and P. Charnay. 1989. Segment-specific expression of a zinc-finger gene in the developing nervous system of the mouse. *Nature.* 337:461–464.

Wilkinson, D.G., S. Bhatt, and B.G. Herrmann. 1990. Expression pattern of the mouse T gene and its role in mesoderm formation. *Nature.* 343:657–659.

Yamamoto, M., C. Meno, Y. Sakai, H. Shiratori, K. Mochida, Y. Ikawa, Y. Saijoh, and H. Hamada. 2001. The transcription factor FoxH1 (FAST) mediates Nodal signaling during anterior-posterior patterning and node formation in the mouse. *Genes Dev.* 15:1242–1256.

Yan, Y.T., J.J. Liu, Y. Luo, C. E, R.S. Haltiwanger, C. Abate-Shen, and M.M. Shen. 2002. Dual roles of Cripto as a ligand and coreceptor in the nodal signaling pathway. *Mol. Cell. Biol.* 22:4439–4449.

Yeo, C., and M. Whitman. 2001. Nodal signals to Smads through Cripto-dependent and Cripto-independent mechanisms. *Mol. Cell.* 7:949–957.

Zhang, J., W.S. Talbot, and A.F. Schier. 1998. Positional cloning identifies zebrafish one-eyed pinhead as a permissive EGF-related ligand required during gastrulation. *Cell.* 92:241–251.